HHS Public Access

Author manuscript

ACS Sens. Author manuscript; available in PMC 2017 May 17.

Published in final edited form as:

ACS Sens. 2016 May 27; 1(5): 488–492. doi:10.1021/acssensors.6b00003.

Simple and Versatile Detection of Viruses Using Anodized Alumina Membranes

Pavan Chaturvedi[†,‡], **Stacy D. Rodriguez**[§], **Ivan Vlassiouk**[‖], **Immo A. Hansen**[§], and **Sergei N. Smirnov**[†,*]

[†]Department of Chemistry and Biochemistry, New Mexico State University, Las Cruces, New Mexico 88003, United States

[‡]Department of Physics, New Mexico State University, Las Cruces, New Mexico 88003, United States

[§]Department of Biology, New Mexico State University, Las Cruces, New Mexico 88003, United States

[‖]Oak Ridge National Laboratory, Oak Ridge, Tennessee 37831, United States

Abstract

A simple sensor for viral particles based on ionic conductivity through anodized alumina membranes was demonstrated using MS2 bacteriophage as an example. A facile two-point measuring scheme is geared toward realization using a computer's sound card input/output capabilities suitable for a fast and inexpensive point of care testing. The lowest detection concentration down to ~7 pfu/mL and a large dynamic range up to ~2000 pfu/mL were obtained due to physical optimization that included proper length and diameter for the pores, removing the oxide layer at the electrode, as well as the chemical optimization of covalent binding of antibodies to the pore's walls.

Graphical abstract

[*]**Corresponding Author**. snsm@nmsu.edu. Phone: 575-646-1547. Fax: 575-646-2649.

ASSOCIATED CONTENT

Supporting Information

The Supporting Information is available free of charge on the ACS Publications website at DOI: 10.1021/acssensors.6b00003.

Extended methods section, SEM images, effect of pH, calculations of the packing efficiency, and impedance measurements using sound card (PDF)

The authors declare no competing financial interest.

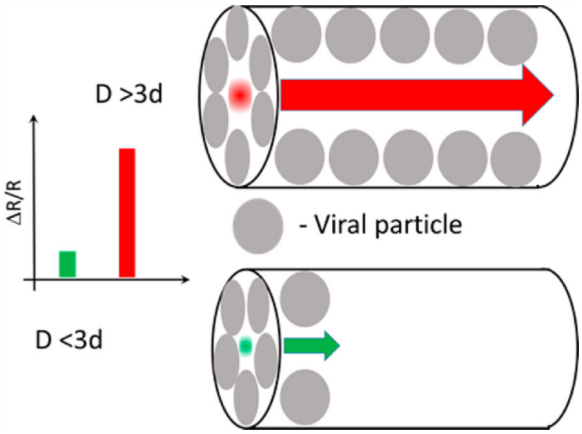

Keywords

AAO; biosensor; virus sensor; MS2; ionic conductance; volume exclusion effect

There has been great interest in recent years in the development of biosensors based on the utilization of nanopores. Various realizations of such sensors employ different mechanisms of detection, from optical[1–3] to electrical,[4–24] in the form of single pores or multiple pores (i.e., nanoporous membranes). Most of these detection schemes typically have the nanopore walls equipped with ligands responsible for specific binding of the specific analytes.

The electrical detection schemes have been typically realized in the form of electrochemical sensors, where the signal from redox species is measured using a potentiostat,[5] but more simple detection approaches based on measurements of ac or dc ionic current have also been demonstrated.[6–17] The pulsed resistance method employing a single pore and detecting the dc current changes has been vastly improved in recent years, especially in the field of DNA sequencing,[6–9] but its application to other bioanalytes is not obvious and the requirement for sophisticated devices needed for fast time detection makes it not very cost-effective.

Techniques where nanopores are equipped with specific ligands (or antibodies) are currently more suitable to broad applications. In this approach, two mechanisms are responsible for the change of ionic current, the long-range electrostatic interactions (surface charge effect) and the steric hindrance (volume exclusion effect).[6–21] Depending on the analyte to be detected, one of these effects can be enhanced by selecting appropriate conditions. In very small diameter nanopores, steric hindrance induced by the captured analyte molecules of the comparable size causes an increase in ionic resistance proportional to the excluded volume of the nanopores and further enhanced by the possible decrease of ionic mobility.[17–21] The equilibrium concentration of ions inside these pores may be affected by the charges on the nanopores' walls, but it is insignificant if the electrolyte concentration is high. If the electrolyte concentration is low and the surface charge is nonzero, the concentration of counterions in the pores may exceed the ion concentration in the outside solution due to the electrical neutrality requirement. The surface charge change brought by the analyte molecules attached to the ligands on the walls under such conditions can be used for their detection.[6,11–15] The effect can be further controlled by adjusting the pH of the electrolyte.

Among the different methods of preparing nanopore arrays or nanoporous membranes, fabrication by anodization of aluminum or titanium is one of the most convenient methods as it does not require a cleanroom or any lithographic techniques. Anodized aluminum oxide (AAO) membranes can be fabricated with controllable pore length and diameter by proper choice of the anodization voltage, the type of electrolyte, the time of anodization, and post treatment. The pore walls can be chemically modified to incorporate the desired ligands to be used for binding of specific bioanalytes.[16–22] Sensors based on AAO membranes have previously been used for detection of small molecules and ions,[22] DNA,[2–4,10,11,17] proteins,[1,2,16,18–21] and viruses.[23,24]

We suggest that this platform is particularly suited for the detection of viruses and can be developed into a fast and inexpensive point-of-care test.

Viruses are infectious agents of small size and simple composition and vary in diameter from 20 nm to 250–400 nm with distinctive shapes. These dimensions are in the range of what can be easily manufactured in AAO membranes. The predominant shapes of viruses are of two kinds: rods/filaments and spheres, which are actually 20-sided (icosahedral) polygons. The larger and more-complex viruses, however, combine both filamentous and polygonal shapes.

MS2 bacteriophages are single-stranded RNA viruses that infect *E. coli*, a Gram-negative bacteria, often used in molecular biology.[25,26] It is a model virus that can be used to mimic other harmful viruses with similar physical structure and properties. The most commonly used methods for detection and identification of viruses are virus culture, polymerase chain reaction (PCR), and enzyme-linked immunosorbent assay (ELISA). These methods are complicated and time-consuming.[27–29] Recently developed electrochemical methods hold much promise due to their low cost, scalability, low power consumption, and good sensitivity. Electrochemical impedance spectroscopy (EIS) is one of such electrochemical detection schemes, which relies on the surface properties of electrodes altered upon binding of a biological analyte. It has been applied for virus detection using flat electrodes[30–34] and AAO membranes.[23,24] Unfortunately, in these studies no clear understanding of the detection mechanism was offered.

Here we elucidate the main features of an AAO-based sensor for viruses and demonstrate through the example of detection of MS2 bacteriophage how such optimization can lead to the lowest detection ~7 pfu/mL with good sensitivity and specificity. The proposed low-cost label-free sensor is simple in production and operation (does not require a potentiostat), which makes it highly suitable for the development of point-of-care applications.

The details on sample preparation are given in the Supporting Information (sections 1–3). Briefly, high-purity Al sheets were anodized in 3 wt % oxalic acid at 4 °C with 60 V DC for 315 min to produce alumina nanoporous membrane using the so-called “two-step” method. It resulted in an almost hexagonal periodic arrangement of the pores with 73 ± 14 nm diameter and 30 μm length, as shown in Figures S2–S4. Etching in 5% phosphoric acid at room temperature for 50 min partially dissolved the oxide layer at the bottom of the pores and also widened the pores to a diameter of 97 ± 17 nm. The membranes remained on the Al

sheet that provided the necessary support for direct mounting in the cell while serving as an electrode. In the alternative approach, the anodization was finished by thinning the alumina barrier layer with stepwise lowering of the current (electroetching; see Figure S1).

To make a sensor for MS2, each anodized membrane was modified by covalent attachment of MS2-phage polyclonal antibody, as illustrated in Scheme S1, and assembled into a cell made of 1-cm-thick Teflon or PDMS with a 5 mm hole on top of the membrane electrode (see Figure S5). The impedance measurements were performed in the two-electrode configuration using a CH Instruments 700C potentiostat with the second electrode being a 1.3 mm Pt on top of and in close contact with the membrane. The impedance spectra were measured at room temperature with no DC bias under 10 mV of AC potential within the frequency range of 1 Hz to 100 kHz using 1× PBS buffer (pH 7.4). The MS2-bacteriophage binding assays were performed in the assembled cell by placing 60 μL of the desired concentration of MS2 (or Qβ) in PBS onto the membrane for 1 h followed by replacing the solution with 1× PBS.

The proposed technique for convenient and accurate detection of various viruses is illustrated here on a representative bacteriophage, MS2, and is based on the volume exclusion mechanism, i.e., increase in the ionic pore resistance due to specific binding of the analyte virus on the pore walls. The optimized design has to address a few important parameters. First, the pores have to be sufficiently long to make their AC ionic resistance detectable. To illustrate the effect let us consider Figure 1 with the Bode plot (the impedance as a function of frequency). The cartoon inset represents the elements contributing to the impedance. Each pore is open on one side to solution and is terminated on the other side by an oxide barrier on top of the aluminum electrode. Since the detection is performed in the two electrode scheme, the counter electrode is similarly important. Typically we use a platinum counter electrode touching the pore entrance but, alternatively, two identical membranes can be used as the electrodes. The equivalent circuit is represented by the oxide barrier part given by the (practically infinite) resistance, R_{ox}, in series with its capacitance, C_{ox}, which are connected to similar elements for the pores, R_{pore} and C_{pore}. The circuit is terminated with the resistance of the solution between the membrane and the counter electrode, R_{sol}. The latter is recognizable only at the highest frequencies and can be ignored. The remaining three elements, C_{ox}, R_{pore}, and C_{pore}, define the appearance of the Bode plot for absolute impedance, $|Z(\nu)|$, as a function of frequency, ν, as well as the phase shift, which is not shown. Each of the capacitances are responsible for the $1/\nu$ varying parts (i.e., the negative slope −1 in the log−log plot) in the low and high frequency ranges, while R_{pore} is responsible for the horizontal portion (where the phase is also close to zero). In order to measure the changes in this resistance effectively, the two capacitances have to be significantly different, by orders of magnitude. That can be achieved by increasing the pore length and by minimizing the impedance of the oxide layer. We achieved the latter by etching in 5% phosphoric acid that leads to almost uniform removal of the oxide layer throughout the whole length of the pores and thus narrowing the oxide barrier and simultaneous pore widening. The latter simultaneously slightly decreases the pore resistance, R_{pore}, and the inverse capacitance, $1/C_{pore}$. The 30-μm-long pores, together with narrowing the oxide layer, provided sufficient enough contrast between C_{pore} and C_{ox} for easy detection of R_{pore}. In the alternative approach, the etching was performed

electrochemically, which did not affect the pore diameter and only minimized the oxide layer.

The second part of optimization involves the pore diameter. The ionic resistance increases proportionally to the excluded volume (presuming that the diffusion coefficient of the ions does not change) and thus the pores' diameter, *D*, needs to be close to the size of the targeted analyte,[35,36] MS2 bacteriophage in our case, which has an almost spherical shape with diameter $d \sim 27$ nm.[37] At the same time, if the pore diameter is too close to that of the analyte and does not satisfy the condition

$$D - 2d > d \quad (1)$$

the analyte binding at the pore entrance would block access to the remaining portion of the pores (see inset in Figure 1A). For that reason, we chose the larger pore diameter of ~97 nm which better matches the condition of eq 1 for MS2. The antibodies attached to walls also have finite size (from ~5 to ~12 nm, in different directions) and one has to take it into account for correct estimation of the free pore diameter, *D*. The separation by size of viruses can be an additional tool for amplifying the sensitivity of such sensors. Figure 1 illustrates that a more efficient removal of the oxide layer in the 73 nm pores led to a smaller capacitive impedance, but the pore resistance was larger than for 97 nm pores of the same length. More importantly, for the sensor based on the smaller diameter pores (73 nm) the condition of eq 1 were not satisfied and the observed membrane pore resistance change due to MS2 binding was smaller almost by a factor 3. The fact that the ratio is not much greater is caused by the viral particles' spreading through the pores well beyond the entrance despite the formal failure of eq 1. One obvious reason for that is a broad variation of the pore diameters; indeed, it is 73 ± 14 nm, which in some places is greater than 2*d*. A slow binding rate of the viral particles with the surface antibodies can also accommodate intrusion of particles beyond the entrance.

It is important for a sensor to be specific to the desired analyte and have a low response to other viruses. As seen in Figure 2, our sensor equipped with MS2 antibodies has negligible response to another bacteriophage of a similar size, Qβ. The relative resistance change for nontargeted phage is smaller by a factor of ~15. The nonzero effect is due to nonspecific binding of the viral particles and can be likely improved by using more effective ligands, rather than polyclonal antibodies. Another possibility of a false reading can arise in mixed samples from physical trapping of the nontargeted viral particles inside the pores by targeted viral particles attached to walls. This undesired effect, again, can be eliminated by using larger pores, e.g., 97 nm, where such entrapment is minimal.

The nature of the volume exclusion effect is such that it should not be affected by the charge on the analyte species or the concentration of ions in the electrolyte or by pH. The competitive surface charge effect[4,6–15] is most strongly present at low electrolyte concentrations. Thus, in our detection scheme a sufficiently high electrolyte concentration was used, ~0.15 M (1× PBS). As shown in SI Figure S6, the effect of pH under such conditions is indeed minimal. As Figures 1 and 2 demonstrate, the AAO-based ionic

resistance sensor with 97-nm-diameter pores shows a significant resistive response for MS2 phage. The impedance measured at 9.6 kHz is primarily due to the membrane pore resistance (a plateau in Figure 1) which changes almost perfectly logarithmically in the concentration range of 10–2000 pfu/mL of MS2. Note that all the measurements in Figures 1 and 2 were performed in the two-point measuring scheme.

If one assumes for simplicity that the diffusion coefficient of ions inside the pores does not change much due to confinement, the maximum increase of the ionic pore resistance can be estimated as the excluded volume arising the bound phages. For tightly packed spheres of diameter d, representing our viral particles on the walls of cylindrical hole with the diameter, $D \sim 3d$, the maximum relative resistance change should be $\Delta R/R \sim \Delta V/V \sim 0.5$ (see Figures S7 and S8 for details), which is close to the experimental value in 97 nm pores, ~47%. The presumption that the diffusion coefficient of ions is not changing inside the pores is an oversimplification[4] and, if included here, should cause the effect to exceed 50%.

The lowest detection concentration measured as an intercept for the optimal device with 97 nm pores in Figure 2, is ~7 pfu/mL when only MS2 was used. When the 1:1 mixtures of MS2:Qβ were used (solid rhombs), the lowest detection concentration for MS2 grew to ~30 pfu/mL and the signal saturated at a slightly lower value of $\Delta R/R \sim 43\%$. Both effects are likely due to nonspecific binding of Qβ, which gets trapped between the MS2 phages but washes off easily, thus the lower signal. The increase in the lowest detection by more than a factor of 2 can be rationalized by a higher diffusion coefficient of Qβ, which is a slightly smaller phage (26 nm vs 27 nm of MS2). The high concentration saturated value, $\Delta R/R \sim 43\%$, in the mixture sample increases further to $\Delta R/R \sim 45\%$ (empty rhomb) when solely MS2 was added. All these suggest that a multistep washing and mixing during incubation can further improve the sensor performance in real samples.

As illustrated in the SI (see Figure S9), this unsophisticated two-point measuring scheme for impedance measurements can be easily realized using a computer's sound card input/output capabilities with accuracy better than 0.5%, more than necessary for accurate signal detection.

CONCLUSION

We have designed a simple ionic conductivity sensor for MS2 phages based on anodized alumina membranes and demonstrated how such sensors can be optimized for other viral particles. Besides the specificity of antibodies, the physical optimization includes the removal of the oxide layer at the electrode and identification of the proper length and diameter for the pores. In particular, the pore diameter has to exceed 3 times the diameter of analyte and the pore length has to be long enough to ensure a significant contrast between the capacitances of the membrane and of the residual oxide layer. The resulting sensor for MS2 bacteriophages has logarithmic dependence in the concentration range of 10–2000 pfu/mL. The lowest detection concentration was ~7 pfu/mL with pure MS2 and ~30 pfu/mL in the 1:1 mixtures of MS2:Qβ that mimic real systems. This simple two-point measuring scheme can be realized using a computer's sound card input/output capabilities which makes it attractive for fast and quantitative point of care testing applications.

Supplementary Material

Refer to Web version on PubMed Central for supplementary material.

Acknowledgments

This work was partially supported by grant from the National Institute of Health (R15-EB-016401-01). The authors are grateful to Dr. P. Cook for help with SEM and Dr. C. Bruce for lending some equipment. A portion of this research was conducted at the Center for Nanophase Materials Sciences, which is a DOE Office of Science User Facility.

REFERENCES

1. Lau KHA, Tan LS, Tamada K, Sander MS, Knoll W. Highly Sensitive Detection of Processes Occurring Inside Nanoporous Anodic Alumina Templates: A Waveguide Optical Study. J. Phys. Chem. B. 2004; 108:10812–10818.
2. Vlassiouk I, Krasnoslobodtsev A, Smirnov S, Germann M. 'Direct' Detection and Separation of DNA Using Nanoporous Alumina Filters. Langmuir. 2004; 20:9913–9915. [PubMed: 15518473]
3. Takmakov P, Vlassiouk I, Smirnov S. Application of Anodized Aluminum in Fluorescence Detection of Biological Species. Anal. Bioanal. Chem. 2006; 385:954–958. [PubMed: 16724216]
4. Vlassiouk, I., Smirnov, S. Biosensing using nanomaterials. Merkoçi, A., editor. Vol. Chapter 15. Wiley; 2009. p. 459-490.ISBN 978-0-470-18309-0
5. Santos A, Kumeria T, Losic D. Nanoporous anodic aluminum oxide for chemical sensing and biosensors. TrAC, Trends Anal. Chem. 2013; 44:25–38.
6. Fologea D, Gershow M, Ledden B, McNabb DS, Golovchenko JA, Li J. Detecting Single Stranded DNA with a Solid State Nanopore. Nano Lett. 2005; 5:1905–1909. [PubMed: 16218707]
7. Harrell CC, Choi Y, Horne LP, Baker LA, Siwy ZS, Martin CR. Resistive-Pulse DNA Detection with a Conical Nanopore Sensor. Langmuir. 2006; 22:10837–10843. [PubMed: 17129068]
8. Iqbal SM, Akin D, Bashir R. Solid-State Nanopore Channels with DNA Selectivity. Nat. Nanotechnol. 2007; 2:243–248. [PubMed: 18654270]
9. Smeets RMM, Keyser UF, Krapf D, Wu MY, Dekker NH, Dekker C. Salt dependence of ion transport and DNA translocation through solid-state nanopores. Nano Lett. 2006; 6:89–95. [PubMed: 16402793]
10. Vlassiouk I, Takmakov P, Smirnov S. Sensing DNA Hybridization via Ionic Conductance through a Nanoporous Electrode. Langmuir. 2005; 21:4776–4778. [PubMed: 15896007]
11. Wang X, Smirnov S. Label-Free DNA Sensor Based on Surface Charge Modulated Ionic Conductance. ACS Nano. 2009; 3:1004–1010. [PubMed: 19284734]
12. Karnik R, Castelino K, Fan R, Yang P, Majumdar A. Effects of Biological Reactions and Modifications on Conductance of Nanofluidic Channels. Nano Lett. 2005; 5:1638–1642. [PubMed: 16159198]
13. Stein D, Kruithof M, Dekker C. Surface-Charge-Governed Ion Transport in Nanofluidic Channels. Phys. Rev. Lett. 2004; 93:035901. [PubMed: 15323836]
14. Vlassiouk I, Smirnov S, Siwy Z. Ionic Selectivity of Single Nanochannels. Nano Lett. 2008; 8:1978–1985. [PubMed: 18558784]
15. Chen W, Wu ZQ, Xia XH, Xu JJ, Chen HY. Anomalous Diffusion of Electrically Neutral Molecules in Charged Nanochannels. Angew. Chem., Int. Ed. 2010; 49:7943–7947.
16. Kukwikila M, Howorka S. Nanopore-Based Electrical and Label-Free Sensing of Enzyme Activity in Blood Serum. Anal. Chem. 2015; 87:9149–9154. [PubMed: 26305576]
17. Takmakov P, Vlassiouk I, Smirnov S. Hydrothermally Shrunk Alumina Nanopores and Their Application to DNA Sensing. Analyst. 2006; 131:1248–1253. [PubMed: 17066194]
18. Han C, Hou X, Zhang H, Guo W, Li H, Jiang L. Enantioselective Recognition in Biomimetic Single Artificial Nanochannels. J. Am. Chem. Soc. 2011; 133:7644–7647. [PubMed: 21534617]

19. de la Escosura-Muñiz A, Chunglok W, Surareungchai W, Merkoçi A. Nanochannels for Diagnostic of Thrombin-Related Diseases in Human Blood. Biosens. Bioelectron. 2013; 40:24–31. [PubMed: 22704840]
20. de la Escosura-Muñiz A, Merkoçi A. Nanochannels Preparation and Application in Biosensing. ACS Nano. 2012; 6:7556–7583. [PubMed: 22880686]
21. de la Escosura-Muñiz A, Merkoçi A. Label-Free Voltammetric Immunosensor Using a Nanoporous Membrane Based Platform. Electrochem. Commun. 2010; 12:859–863.
22. Yu J, Zhang L, Xu X, Liu S. Quantitative Detection of Potassium Ions and Adenosine Triphosphate via a Nanochannel-Based Electrochemical Platform Coupled with G-Quadruplex Aptamers. Anal. Chem. 2014; 86:10741–10748. [PubMed: 25333881]
23. Peh AEK, Li SFY. Dengue Virus Detection Using Impedance Measured Across Nanoporous Alumina Membrane. Biosens. Bioelectron. 2013; 42:391–396. [PubMed: 23220066]
24. Cheng MS, Ho JS, Tan CH, Wong JPS, Ng LC, Toh C-S. Development of an Electrochemical Membrane-Based Nanobiosensor for Ultrasensitive Detection of Dengue Virus. Anal. Chim. Acta. 2012; 725:74–80. [PubMed: 22502614]
25. Jończyk E, Kłak M, Międzybrodzki R, Górski A. The Influence of External Factors on Bacteriophages. Folia Microbiol. 2011; 56:191–200. [PubMed: 21625877]
26. Bradford SA, Simunek J, Bettahar M, Van Genuchten MT, Yates SR. Modeling Colloid Attachment, Straining, and Exclusion in Saturated Porous Media. Environ. Sci. Technol. 2003; 37:2242–2250. [PubMed: 12785531]
27. Iqbal SS, Mayo MW, Bruno JG, Bronk BV, Batt Ca, Chambers JP. A Review of Molecular Recognition Technologies for Detection of Biological Threat Agents. Biosens. Bioelectron. 2000; 15:549–578. [PubMed: 11213217]
28. Lazcka O, del Campo FJ, Muñoz FX. Pathogen Detection: A Perspective of Traditional Methods and Biosensors. Biosens. Bioelectron. 2007; 22:1205–1217. [PubMed: 16934970]
29. Perrott P, Smith G, Ristovski Z, Harding R, Hargreaves M. A Nested Real-Time PCR Assay Has an Increased Sensitivity Suitable for Detection of Viruses in Aerosol Studies. J. Appl. Microbiol. 2009; 106:1438–1447. [PubMed: 19191944]
30. Sadik OA, Aluoch AO, Zhou A. Status of Biomolecular Recognition Using Electrochemical Techniques. Biosens. Bioelectron. 2009; 24:2749–2765. [PubMed: 19054662]
31. Caygill RL, Blair GE, Millner PA. A review on Viral Biosensors to Detect Human Pathogens. Anal. Chim. Acta. 2010; 681:8–15. [PubMed: 21035597]
32. Shabani A, Zourob M, Allain B, Marquette Ca, Lawrence MF, Mandeville R. Bacteriophage-Modified Microarrays for the Direct Impedimetric Detection of Bacteria. Anal. Chem. 2008; 80:9475–9482. [PubMed: 19072262]
33. Prieto-Simón B, Saint C, Voelcker NH. Electrochemical Biosensors Featuring Oriented Antibody Immobilization via Electrografted and Self-Assembled Hydrazide Chemistry. Anal. Chem. 2014; 86:1422–1429. [PubMed: 24377288]
34. Prieto-simón B, Bandaru NM, Saint C, Voelcker NH. Tailored Carbon Nanotube Immunosensors for the Detection of Microbial Contamination. Biosens. Bioelectron. 2015; 67:642–648. [PubMed: 25316087]
35. Uehara H, Kakiage M, Sekiya M, Sakuma D, Yamonobe T, Takano N, Barraud A, Meurville E, Ryser P. Size-Selective Diffusion in Nanoporous. ACS Nano. 2009; 3:924–932. [PubMed: 19323485]
36. Boss C, Meurville E, Sallese J-M, Ryser P. Size-Selective Diffusion in Nanoporous Alumina Membranes for a Glucose Affinity Sensor. J. Membr. Sci. 2012; 401–402:217–221.
37. Strauss JH, Sinsheimer RL. Purification and Properties of Bacteriophage MS2 and of its Ribonucleic Acid. J. Mol. Biol. 1963; 7:43–54. [PubMed: 13978804]

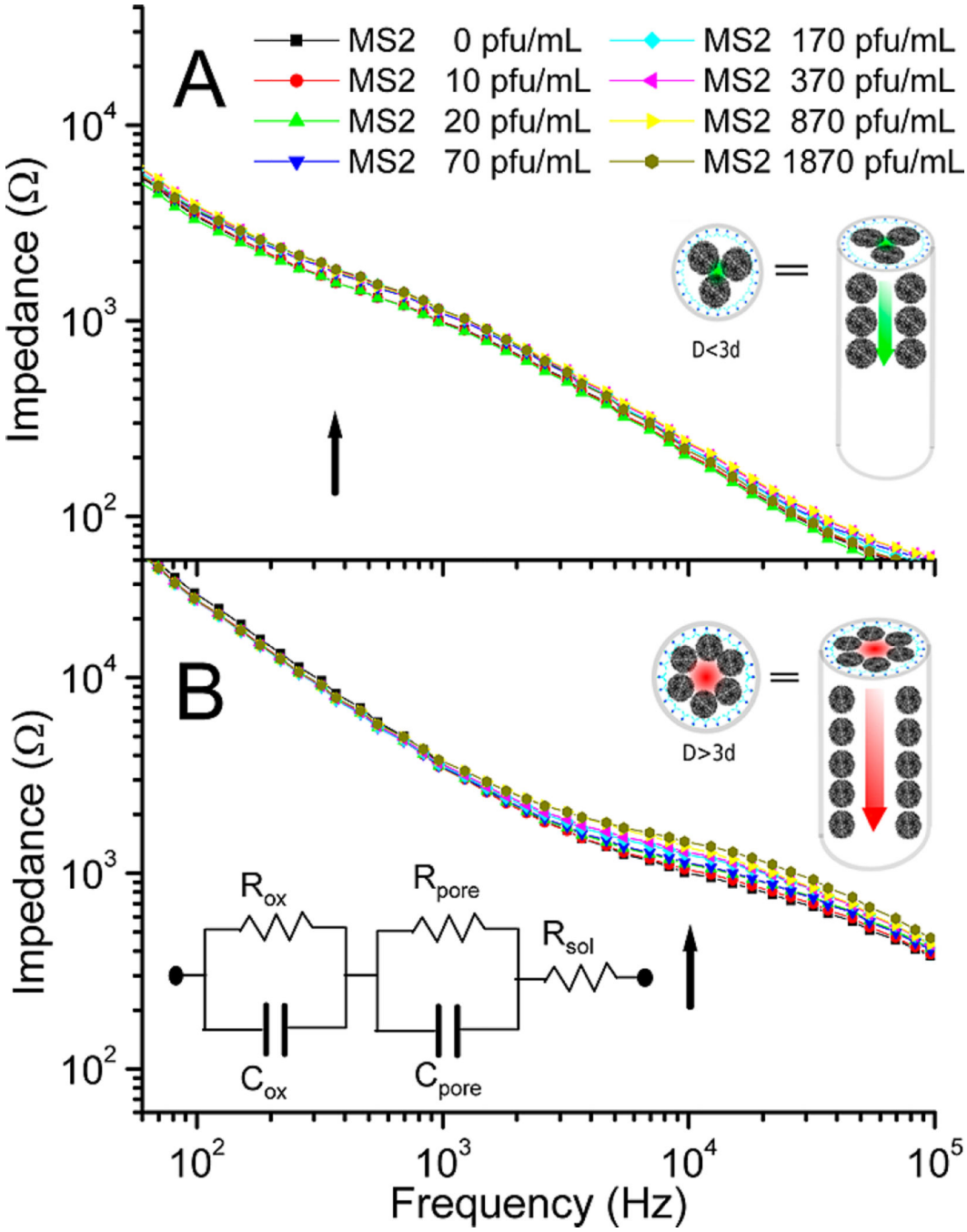

Figure 1.

Bode plots for sensor responses to different concentrations of MS2 bacteriophage. A. The sensor is based on 73 nm pores. B. The sensor is based on 97 nm pores. The arrows in both cases indicate the corresponding frequencies of optimal detection and the insets illustrate that the pores with diameter, $D < 3d$, are less efficient due to compromised accessibility of the walls to viruses with diameter d (A), while larger pores are not affected (B). The inset in B illustrates the effective electrical circuit diagram, where R_{sol} is the resistance of solution

above the membrane, R_{pore} and C_{pore} are the resistance and capacitance of the pores in the membrane, and R_{ox} and C_{ox} are the resistance and capacitance of the oxide layer.

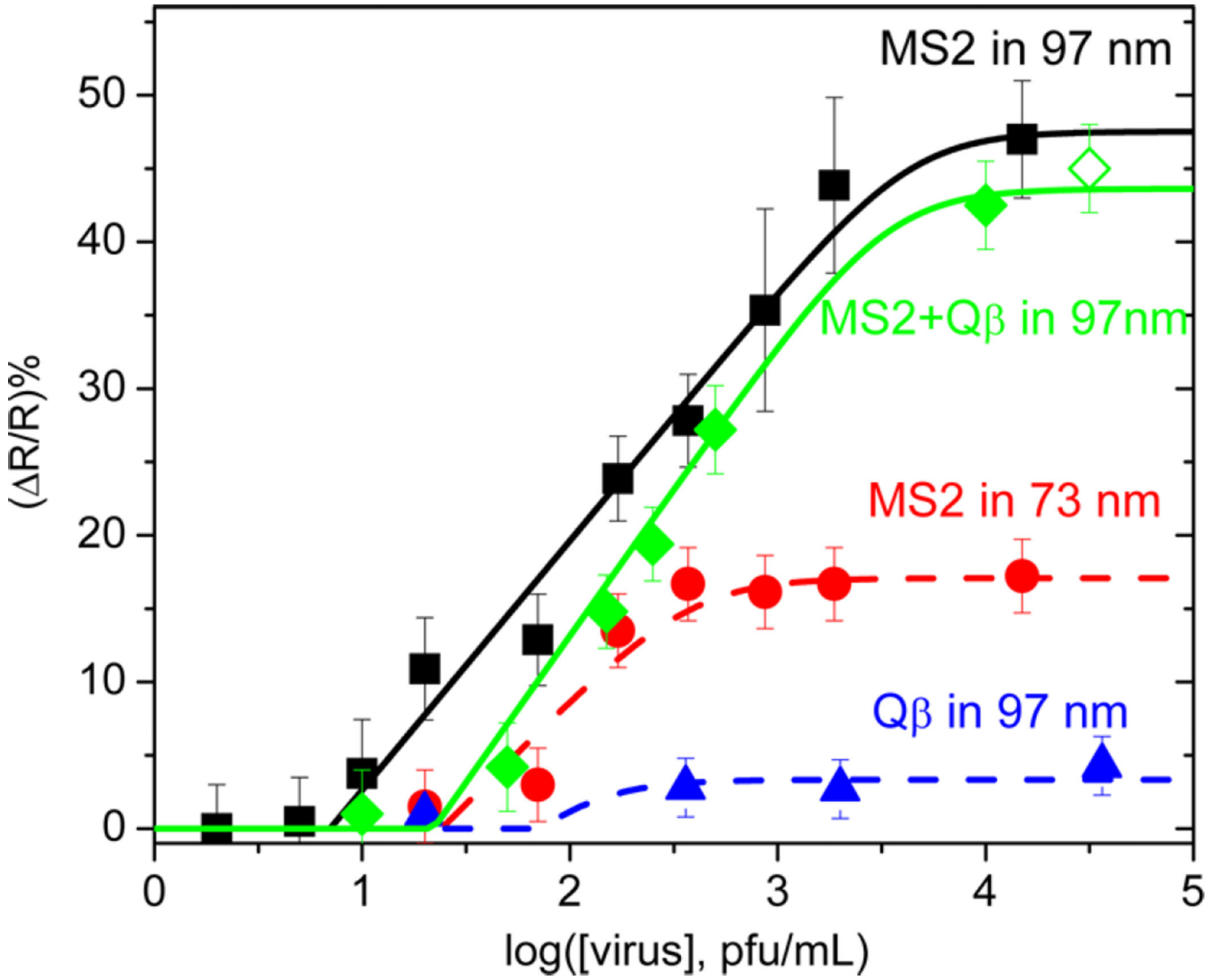

Figure 2.

Change in the sensor's impedance at the resistive part as a function of concentration of viruses (MS2 bacteriophage for squares, circles, and rhombs and Qβ bacteriophage for triangles). All sensors have covalently immobilized antibodies for MS2 in membranes with the same pore length but different pore diameters: 97 nm for squares, triangles, and rhombs and 73 nm for circles. Solid rhombs identify 1:1 mixtures of MS2:Qβ.